Riley Power Inc., a
Babcock Power Inc. company.
www.babcockpower.com

TECHNICAL PUBLICATION

From Bunker to Stack: The Cost-Reduction and Problem-Solving Benefits of Computational Fluid Dynamics For Utility and Industrial Power Generation

by
Kenneth R. Hules, Sc.D.
Senior Principal Engineer, CFD

and

Ali Yilmaz, Ph.D.
Staff Engineer, CFD
Riley Power Inc.
(Formerly Babcock Borsig Power, Inc.)
Worcester, Massachusetts

Presented at
POWER-GEN International 2002
December 10-12, 2002
Orlando, Florida

and

Electric Power 2003
March 4-6, 2003
Houston, Texas

Riley Power Inc.
5 Neponset Street
Worcester, Massachusetts 01606
www.babcockpower.com

T-180

FROM BUNKER TO STACK: THE COST-REDUCTION AND PROBLEM-SOLVING BENEFITS OF COMPUTATIONAL FLUID DYNAMICS FOR UTILITY AND INDUSTRIAL POWER GENERATION

by

Kenneth R. Hules, Sc.D.
Senior Principal Engineer, CFD

and

Ali Yilmaz, Ph.D.
Staff Engineer, CFD
Riley Power Inc.

ABSTRACT

Why is Computational Fluid Dynamics (CFD) an important design and analysis tool for new and existing power plants? Because, in project after project, the ability of CFD to follow the fuel, air, and flue gases through all types of power generation equipment has delivered cost savings, reduced downtime, or quicker turnaround time for the customers.

This paper presents examples of how CFD analysis helped achieve cost savings and/or improved operation in utility and industrial power plants. The examples cover specific hardware components and phenomena in coal and gas fired steam generation plants including:

- *Pulverizers and Classifiers: Simple CFD modeling has led to a better understanding of the classification process in terms of better fineness and product cut-size control as a function of the classifier design and pulverizer operating parameters.*
- *Erosion by Pulverized Coal or Flyash: CFD modeling has solved particulate erosion problems in coal pipes and coal burner heads as well as in economizer bundles modified by the addition of an SCR system.*
- *Low NO_X Coal Burners: CFD modeling has improved burner aerodynamics for better NO_X control and identified initial setup values for low NOx burner retrofits, thus eliminating long and costly burner startup, commissioning, and shakedown periods.*
- *Utility Furnaces with Air Staging Systems: CFD modeling has simplified the design of overfire air (OFA) systems as part of low NO_X burner retrofits in utility boilers. Additionally, CFD models correctly have indicated waterwall zones prone to corrosion because of localized reducing atmospheres, which match historical behavior, as well as demonstrated simple and cost effective boundary air designs to reduce corrosion.*

© Riley Power Inc. 2003

- *Industrial Boilers: Simple CFD models have led to system performance curves for final steam temperature, furnace draft loss, and furnace erosion potential which the plant used to control process steam temperature in a low NO_x burner retrofit. The system performance curves significantly reduced the outage time and testing needed to set the boiler baffle system.*
- *Airheaters to ESPs: CFD modeling yielded baffle and mixer designs in the inlet and outlet ducting of a large multipass tubular airheater which improved the flue gas temperature distribution into an ESP so that fuel switching for cost reduction was possible.*
- *SCR Systems: CFD modeling of SCR inlet ductwork with complicated static mixers reproduced experimental test results of a water spray based flue gas attemperator, and yielded a spray pattern design for maximum gas temperature uniformity and minimum duct wall wetting.*

The paper also notes the economic advantage of CFD analysis in the examples presented.

INTRODUCTION

Although years of experience and expertise have led to proven and effective pieces of equipment for converting fossil fuels to steam, new pollution control demands have raised significantly the performance levels required of most devices in the U.S. electric generating industry. In the past, equipment improvements may have been hard-won by experimentation with full-scale models or field testing, but today's overall economic landscape and pollution control requirements do not allow for such slow and expensive methods of improving existing equipment or designing new systems.

A design and analysis tool fairly new to the power generation industry, yet capable of enormous technical and economic benefit, is computational fluid dynamics (CFD). CFD has come to power generation only recently because of the advent of small, low-cost, but very fast and powerful computers as well as the maturation of CFD numerical methods and mathematical models for physical processes relevant to the power industry. This new tool offers methods to analyze and improve almost all pieces of power generation equipment from fuel handling, fuel preparation, firing systems, furnace flow and combustion behavior, heat transfer performance for steam generation, flue gas processing for emissions control, and overall boiler output. In other words, CFD can have a strong positive economic and technical impact in power generation from fuel bunker to stack. This paper presents recent CFD experiences, focusing on pulverized coal-fired utility boilers and industrial process steam boilers, which illustrate the range of technical applications of CFD in the power field and their cost-saving or revenue-enhancing results.

PULVERIZERS AND CLASSIFIERS

In pulverized coal-fired utility boilers, complete control of coal fineness exiting the mills leads directly to better control of the firing system, the combustion process, lower emissions, lower carbon loss in the flyash, better boiler efficiency, recovered capacity, and reduced operating costs. However, today's coal mills do not always give plant operators complete control of coal fineness, i.e., control of product cut-size as well as mean coal particle size, while limiting mill power requirements and maximizing coal throughput for a given mill size.

Phase I of an ongoing mill improvement project at Riley Power Inc. (RPI), a subsidiary of Babcock Power Inc., used simple CFD simulations of several rotating cage designs retrofitted to a static classifier in a coal mill. This approach quickly gave performance trends for a range of rotor designs and operating conditions. Figure 1 shows CFD results for air flow paths

through the classifier as a function of rotor speed. These plots indicate how the balance of conveying air kinetic energy and rotor centrifugal force shifts, and changes air and coal dust flow direction in the classifier. The more indirect the flow path through the classifier, the greater the classifying effect. Figure 2 shows classifier results in the form of product size-rejection efficiency curves computed from the CFD models, while Figure 3 shows some CFD-predicted product size distributions. The CFD models predicted that when the pulverized coal feed follows a Rosin-Rammler distribution, then the product also has a Rosin-Rammler distribution with cut size as a function of rotor speed. Unfortunately, rotor speed does not change the slope of the distribution curves much to give greater fineness in the form of high product output at small particle size. This project and CFD simulations of dynamic classifiers continues at RPI.

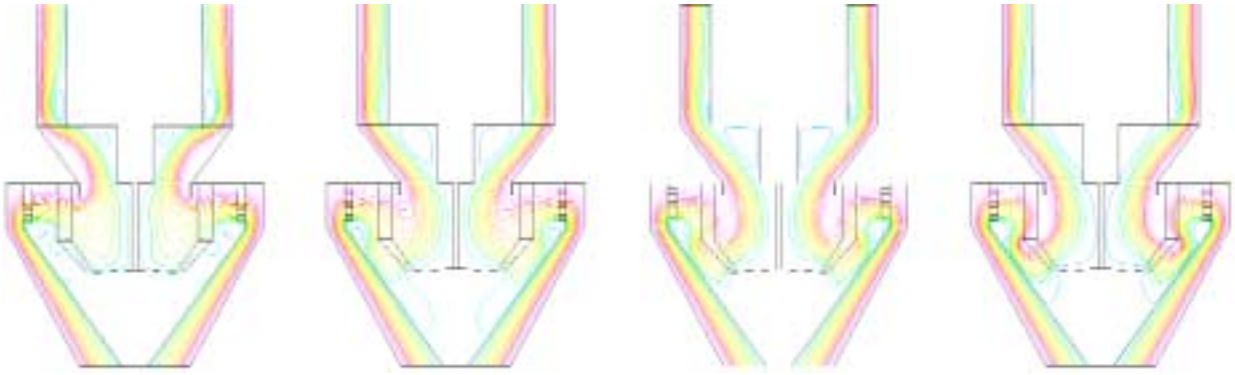

Figure 1 CFD-computed air flow paths within classifier with rotating cage at (a) low speed, (b) below critical speed, (c) above critical speed, and (d) high speed.

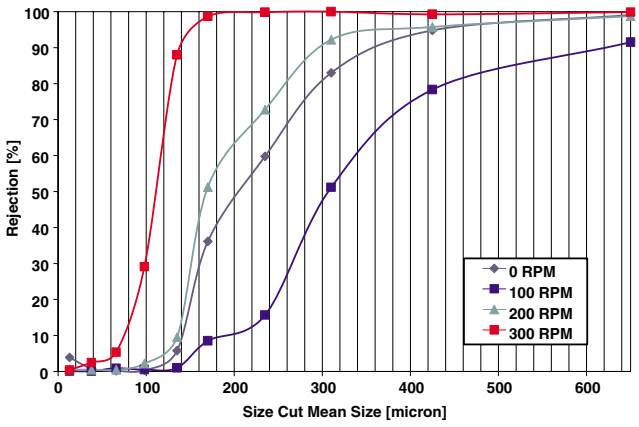

Figure 2 Computed dynamic classifier rejection efficiency from simple CFD models.

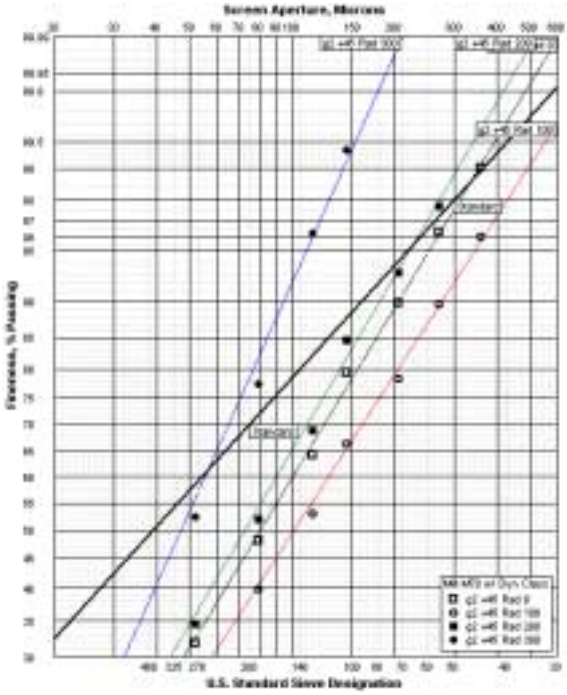

Figure 3 Computed size distributions of mill product from simple CFD models.

The overall goals of the project have been to increase control of the product cut size and overall fineness while improving mill throughput. What do these changes do for our customers? Better control of cut-size and fineness distribution translate directly into better combustion efficiency with lower flyash carbon loss and higher boiler efficiency. An improvement in throughput for a given product distribution means lower power consumption and potentially smaller or fewer mills for a given boiler, which reduces capital and operating costs.

EROSION BY PULVERIZED COAL OR FLYASH

In pulverized coal-fired utility boilers, the pneumatic transport of pulverized coal at the front end and flyash at the backend can create serious erosion problems that lead to unscheduled outages, downtime, lost revenue, and elevated O&M costs. CFD simulations have given very good agreement with field-observed zones of high erosion. Thus CFD has shown itself capable of simulating field conditions so that insight into the origin of a particular erosion problem is obtained. Then CFD simulations with alternate geometries, conditions, and materials are made to find an improvement before expensive field testing is tried.

Figure 4 contains photos of coal burner pieces exhibiting severe erosion from the pulverized coal feed at a large utility boiler. The erosion rate dropped service life well below accept-

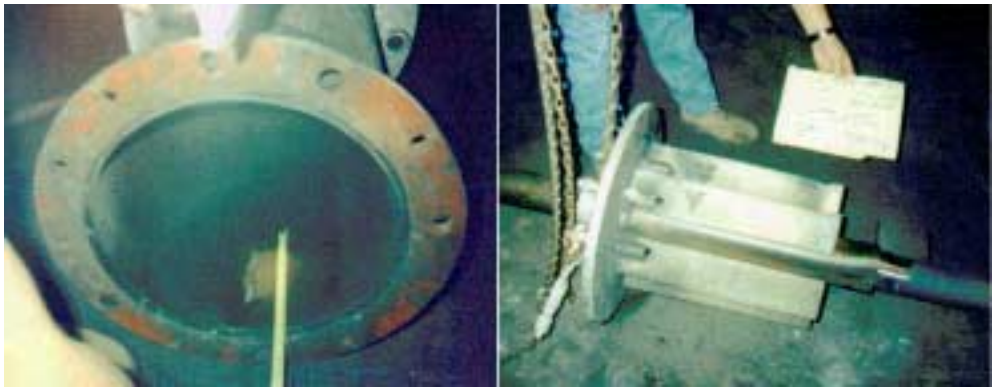

Figure 4 Field documentation of erosion in coal burner spool piece and head vanes.

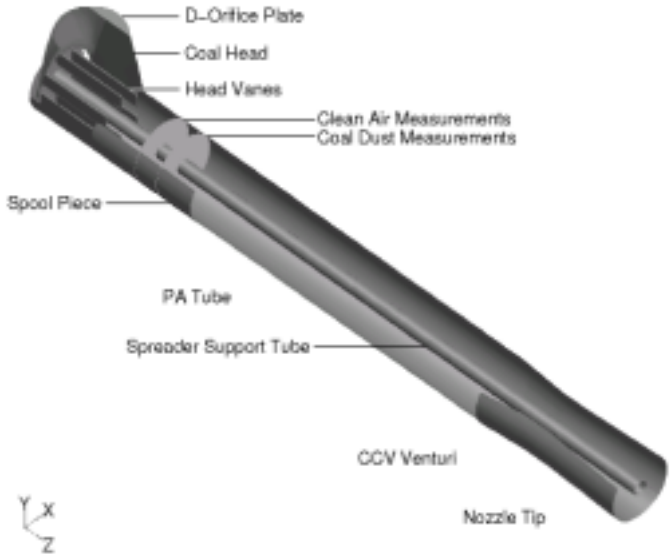

Figure 5 Detail of coal erosion model showing burner and field measurement locations.

able limits. Field testing, including isokinetic particle sampling, investigated the effect of burner head vane settings and coal pipe D-shaped orificing on the erosion and coal dust distribution within the burner. In support of the field testing, CFD models of the final ¼ of the coal pipe run, burner head, and RPI CCV® Burner PA internals were built and run. Figure 5 shows the burner details in the CFD models as well as the field measurement locations.

Figure 6 shows comparisons of the field-measured and computed clean air velocity and coal dust concentration distribution for a burner head and orifice setting in the tests. Overall the computed clean air velocity distribution agrees with the field measurements while the computed coal dust concentration distribution shows only fair agreement with the measured values. It is important to remember that the field measurement of dust in a working burner at a utility boiler is a very difficult, hot, and dirty process that has a relatively high uncertainty in the results.

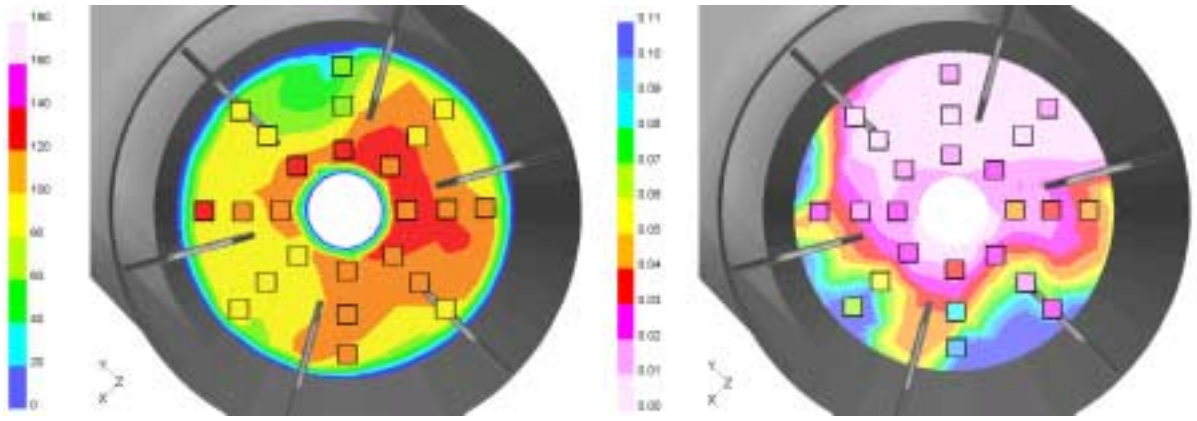

Figure 6 Comparison of field-measured and CFD computed PA velocity and coal dust concentration in a CCV® Burner. (Field data in squares using color scale of computed values.)

Figure 7a shows computed erosion rates in the burner head for the geometry which produced the erosion in Figure 4 while Figure 7b shows results for the settings suggested by the CFD analysis as a good choice for significant erosion reduction. Notice that Figure 7a shows a long erosion gouge in the burner head of similar size, location, and orientation as the erosion gouge in Figure 4 as well as high erosion in similar locations on the burner head vanes. These similarities indicate good agreement of the CFD erosion calculations to the field test. Ultimately, use of the burner head setup suggested by the CFD simulations and improved abrasion resistance materials in these few key locations has extended service life beyond the required minimum.

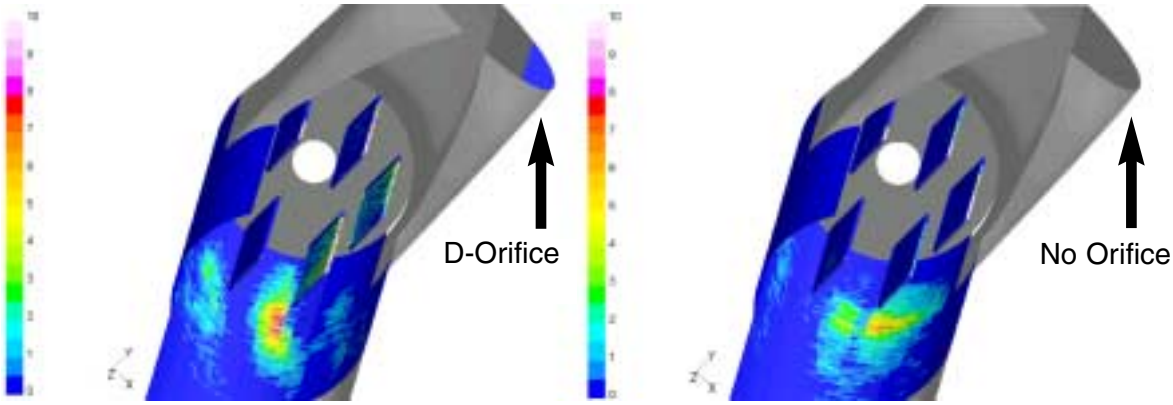

Figure 7a (left) and 7b (right) Computed burner head erosion rates for field and suggested burner head setups.

Attacking and solving a problem like this with CFD analysis only would have saved over $100,000 in field testing costs, plus lost revenues and costs for several outages instead of no outages during the required service life of the burner head replaceable parts.

Unfortunately, erosion does not stop with combustion of the pulverized coal. Flyash from the furnace can be as troublesome as the feed coal. This is especially true when an SCR is installed between the backpass and airheater. In general, SCR operation requires a minimum flue gas temperature for effective NO_X removal. Typically, a flue gas bypass system around all or part of the economizer is necessary to maintain and control flue gas temperature above 600°F at low boiler loads. In some cases this modified backend geometry can distort severely the flue gas flow across the end of the economizer at the bypass entrance, and create much higher localized gas velocities (and therefore erosion potential) than the original economizer design values. CFD studies can determine potential increases in flyash erosion rate at the junction of the flue gas by-pass duct and backpass rear wall. The objective of such a CFD analysis is the development of tube protection strategies for zones of high erosion rate.

In this example, the flue gas bypass location coincided with the top economizer tube bank. Figures 8a and 8b show the detailed 3-D CFD model of a narrow slice of the entire tube bank assembly including the enclosure waterwall tubes that were necessary to model in this case. Mesh generation took time, attention, and the latest meshing features available to account for adequate boundary layer treatment of the multiply curved tubes and give a quality mesh overall. The CFD simulations were steady-state to accommodate the flyash particle tracking calculations used to predict erosion. Flyash particle size distribution was determined from economizer and ESP hopper samples. Additionally, a 1-D boiler backpass heat transfer model was built to calculate the required flue gas bypass flow to reach desired SCR inlet temperatures for a range of low boiler loads. Of greatest interest was the prediction of erosion rate change for a low unit load corresponding to a flue gas bypass operation of 35% of available flue gas flow.

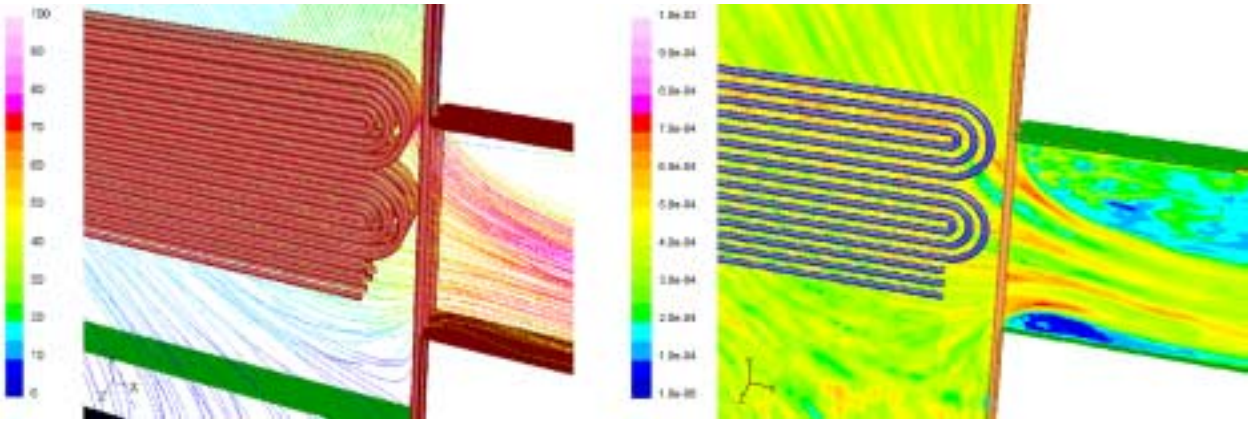

Figure 8a (left) and 8b (right) Flue gas bypass junction model showing predicted gas flow pathlines and predicted flyash concentration.

Figure 9 shows CFD-predicted erosion rates on the economizer enclosure waterwall tubes and economizer tube elbows at the entrance to the bypass. Simple hand calculations of erosion using 1-D experimental correlations with inputs such as superficial flue gas velocity and average flyash particle concentration are not sufficient to predict peak erosion rates indicated by the non-uniform, very localized rates of high erosion predicted in Figure 9. The localized high flyash particle density and gas velocities in Figure 8 and particle impinge-

ment at non-normal angles of contact on the tube surfaces cause higher erosion rates than calculated in the simple correlations. Figure 9 shows increased erosion rates on the leading surfaces of the tubes close to the bypass entrance, especially on the wall tubes and economizer end elbow insides. Based on these results, strategies for protecting the tubes in the limited areas of high erosion rate were formed and rated. To reduce gas velocity, an important parameter in erosion, the gas flow area at the bypass entrance was opened by about 20% by increasing the bypass duct height and adding a chamfer to the duct inlet. Additionally, a portion of the wall tubes and economizer tubes received shields.

In this example the economic benefit of the CFD analysis is harder to quantify simply because CFD was used as a design tool to avoid the anticipated high erosion. The CFD-derived recommendations were implemented before flyash-induced erosion became a problem by forcing an outage and loss of power and revenue production.

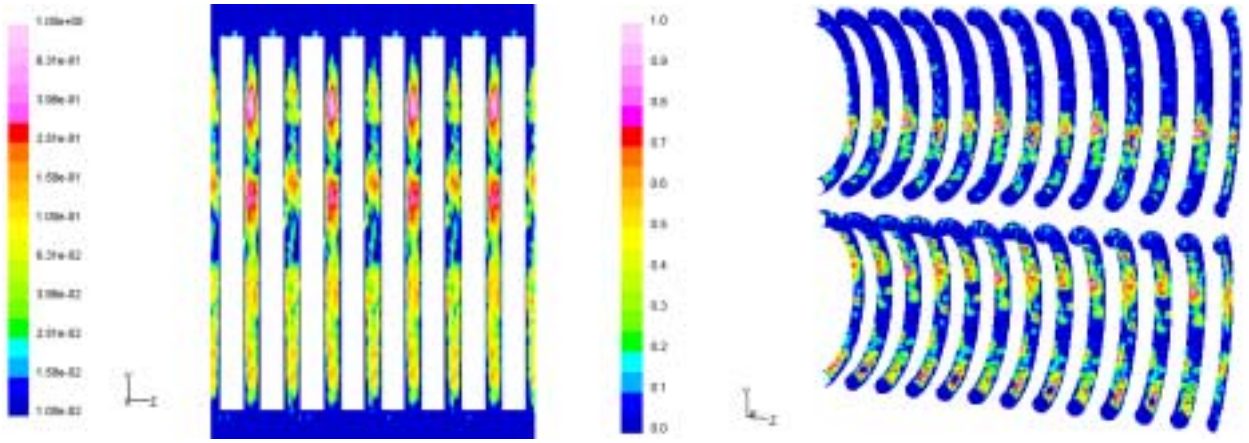

Figure 9 Computed erosion rate results on waterwall tubes and economizer tube ends.

LOW NO_X COAL BURNERS

CFD shines as a tool for developing improvements in utility low NO_X burners whether they are coal, oil, or gas. The state of computational combustion is sufficiently advanced to expect reasonably close calculations of burner flame heat release and temperature distributions as well as real-world issues like flame attachment. Flame attachment is controlled by near-burner flow behavior and falls easily into the scope of CFD burner simulations.

For example, a RPI TURBO® Furnace equipped several years ago with RPI swirl-stabilized TSV® burners, firing Eastern bituminous coal, was not making the required NO_X values. The unit was limited to 95% load to remain in compliance. Additionally, direct observation through viewports confirmed flame detachment was occurring, which affected operations as a loss of flame scanner signal and occasional fuel trips and unit shutdowns. A series of CFD simulations explored possible burner modifications to regain flame attachment along with a flame internal recirculation pattern known to reduce NO_X significantly in RPI single register and dual air zone CCV® Burners. Figure 10a shows the computed temperature distribution in cross-sections through the flames for the original burner while Figure 10b does the same for the TSV® burner modified according to the best results of the CFD explorations. Direct observation through the furnace viewports confirmed that the flame shape and flame detachment shown in Figure 8a are in very good agreement with the actual flames. This increased confidence that the CFD modeling was reasonable and the CFD results for a modified burner would be matched by field behavior.

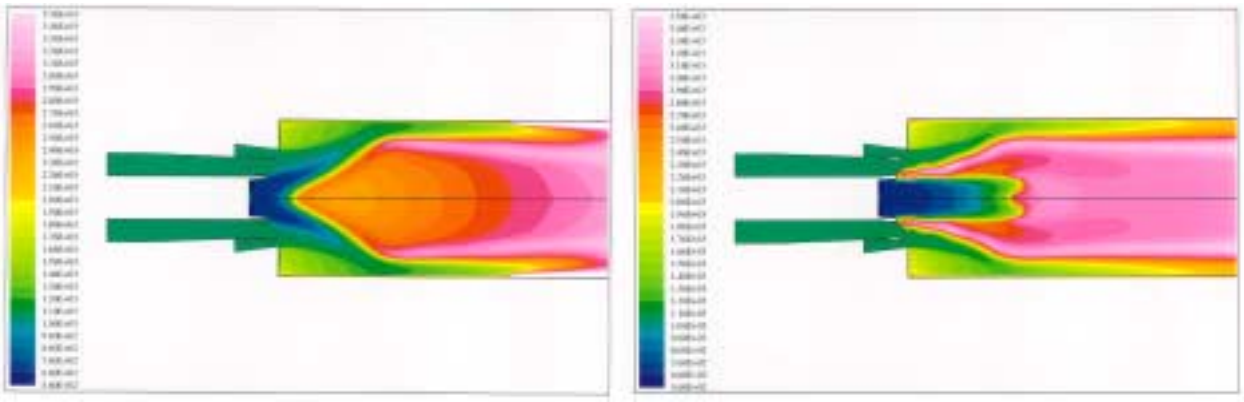

Figure 10a (left) and 10b (right) CFD-computed temperature distributions for original and modified TSV® Burners.

Compared to the original burner (Figure 10a), the modified burner (Figure 10b) adds only three parts of relatively simple construction, low cost, and ease of installation. The modifications required no laboratory testing. The design from the CFD process went directly to production and installation. The design had to work the first time after installation, and in fact, the unit restarted with positive results. The tightly attached flame shape shown in Figure 10b appeared in the furnace viewports. The flames were very stable and scanner signal intensity consistently came in at 97%to 100% from full load down to 35% load. The flames were so well attached to the burner tips that they could not be detached by any changes in burner settings or unit operating conditions. More importantly, the unit recovered capacity even as the NO_X emissions dropped 10% to fall comfortably below the specified value at loads exceeding 100% MCR.

In this extreme case, simple 2-D CFD modeling saved many thousands of dollars of burner testing while cutting development time to a few weeks for several major types of design options. The CFD development process created a simple and cost-effective new burner with low NO_X production and strong, stable flames for tough retrofit applications. Finally, the CFD-improved burners restored significant unit capacity while providing a cushion against NO_X limitations.

CFD value added to burners extends beyond the design phase and into unit operations. For example, plug-in low NO_X burner retrofits require proper control settings to meet boiler performance guarantees. Typically in retrofit projects, boiler performance guarantees require maintaining pre-retrofit boiler efficiency, main steam and reheat temperatures, and windbox-to-furnace pressure differentials while meeting guarantee NO_X and CO emissions and flyash LOI values.

As in the example above, simple 2-D single burner CFD models, now employing only aerodynamics, become a cost-effective design tool to predict burner settings necessary to achieve optimum near-burner aerodynamics for low NO_X emissions and low LOI as well as estimate changes in flame length and attachment. The CFD results highlight the type and location of the flame structure's internal recirculation zone (IRZ). Aerodynamic interactions of swirling air flows leaving the burner dominate the control of IRZ characteristics. Near-burner aerodynamics relate qualitatively to flame behavior (e.g., flame length and attachment), LOI, and NO_X emissions when coupled with full-scale burner combustion test results.

Figure 11 shows the predicted near-burner IRZ for a RPI low NO_X coal-fired dual air zone CCV® Burner at three tertiary air (TA) vane settings. The computed streamlines for low TA angle indicate that two near-burner flow recirculation zones exist: a) an external

recirculation zone (ERZ) driven by secondary air (SA), and b) an IRZ driven partially by primary air (PA). The PA-driven IRZ is essential for establishing a fuel rich zone during the initial combustion process, good flame attachment, and low flyash LOI. Figure 11 indicates that the PA-driven IRZ diminishes as TA vane angle increases, resulting in less coal particle capture by the IRZ and increased flyash LOI values. To the right of the CFD results in Figure 11 are actual burner optimization test data on flyash LOI and NO_X emissions. The test data agree well with the indications in the CFD predictions, i.e., LOI is lowest for a strong PA-driven IRZ at low TA angles while flyash LOI sharply increases as the PA-driven IRZ disappears at high TA angles.

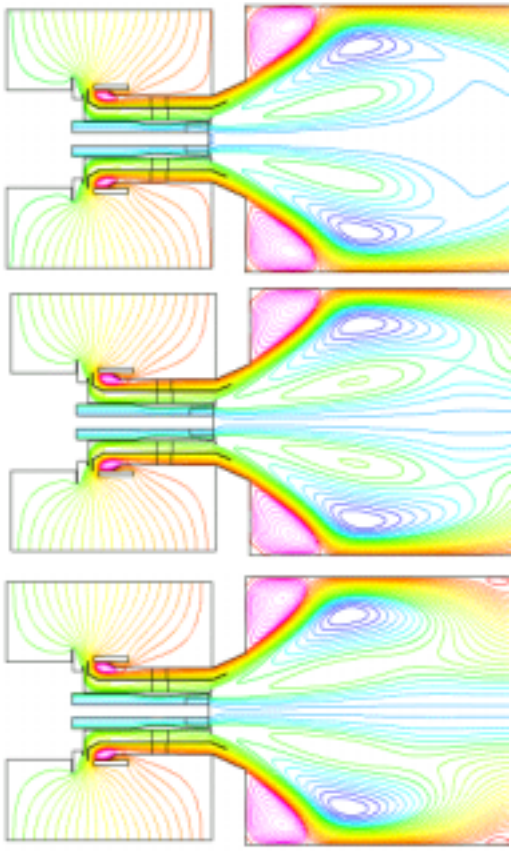

TA Vane Angle (Degrees)	UBC (%)	NO_X (lb/MMBtu)
30	7.89	0.397
35	8.48	0.354
40	13.33	0.368

Figure 11 Comparison of CFD predictions of near-burner flow behavior and burner performance test data of LOI and NO_X emissions for a front wall-fired utility boiler.

CFD modeling also can predict burner settings to achieve optimum near-burner aerodynamics. These predictions expedite low NO_X burner tuning efforts and boiler commissioning in both new boiler and burner retrofit projects. Table 1 compares burner settings and performance from CFD-derived recommendations and field test results for three recent RPI dual air zone low NO_X coal-fired CCV® Burner retrofit projects. The field test results are final burner settings for the performance guarantee tests at peak unit loads. All three retrofit projects met all the performance guarantees with minimal burner tuning efforts (more than a 50% reduction in testing and setup time).

In these cases the economic value of CFD is obvious and very real. CFD predictions of burner settings for startup can trim two to three weeks off burner tuning duration and boiler commissioning. Not only do startup and commissioning costs go down many thousands of dollars, the unit produces full power and revenue during what would have been testing and tuning time.

Table 1 Comparison of CFD-recommended burner settings and finalized burner settings from peak load guarantee setting.

Furnace Type	Cell-Fired Supercritical		Front Wall-Fired Subcritical		Opposed Wall-Fired Subcritical	
Number of Burners	40		16		56	
Data Source	CFD Results	Accept Test	CFD Results	Accept Test	CFD Results	Accept Test
SA Damper Opening (in)	1.750	1.875	1.25	1.25	1.25	1.25
Avg. Shroud Opening (%)	60	67	60	50	59	63
TA Vane Angle (°)	30	30	30-35	35	30	35
PA Coal Spreader Setback (in)	1	1	1	1	1	1
dPwindbox-furnace (iwc)	4.00	4.10	4.50	4.57	3.25	3.75
Avg. SA/TA Flow Ratio	0.50	0.46	0.51	0.59	0.50	0.51

UTILITY FURNACES WITH AIR STAGING SYSTEMS

Beyond the intricacies of burners, a utility furnace is a complex energy and chemical plant in its own right. Requirements for efficient conversion of fuel energy into electricity and creation of minimal emissions within a reliable and cost-effective shell do not always go hand-in-hand. Today, to achieve emissions goals, even low NO_x burners may need other front-end combustion system modifications such as air staging, i.e., overfire air (OFA), a proven NO_x reduction technique suitable for retrofit to utility furnaces. However, even while following some general design principles, a retrofit OFA system is a one-of-a-kind installation if it seeks to deliver maximum performance in terms of low NOx, final O_2 distribution, low LOI, and minimal impact on furnace exit flue gas temperature distribution.

Since this is now a mixing problem in addition to the combustion chemistry, such projects typically invoke large 3-D CFD models of the entire utility furnace and part of the convective backpass. Figure 12 displays the 3-D CFD model geometry for an opposed wall-fired furnace of 600 MWg capacity firing PRB coal. Figure 12 shows CFD results for a base case model with the burners and firing system before new burner and OFA retrofit. Plots a) and b) display computed gas temperature and O_2 concentration distributions throughout the furnace volume while plots c) and d) show computed sidewall heat flux and sidewall O_2 levels respectively. In this project, model validation came through a series of base cases with variations in mills and burners out of service according to historical practice and a comparison of CFD-computed furnace exit gas temperature (FEGT) with calculations of actual furnace performance.

RPI's approach for attaining the NO_x reduction was a retrofit of new dual air zone CCV® Burners in a more compact firing pattern in the lower furnace to give space in the upper furnace for the OFA ports and sufficient residence time for burnout. Following the layout of Figure 12, Figure 13 shows the computed performance for the system design selected after several CFD trials of alternate approaches. This installed design created minimal FEGT increase, as required, while meeting all performance guarantees immediately upon startup.

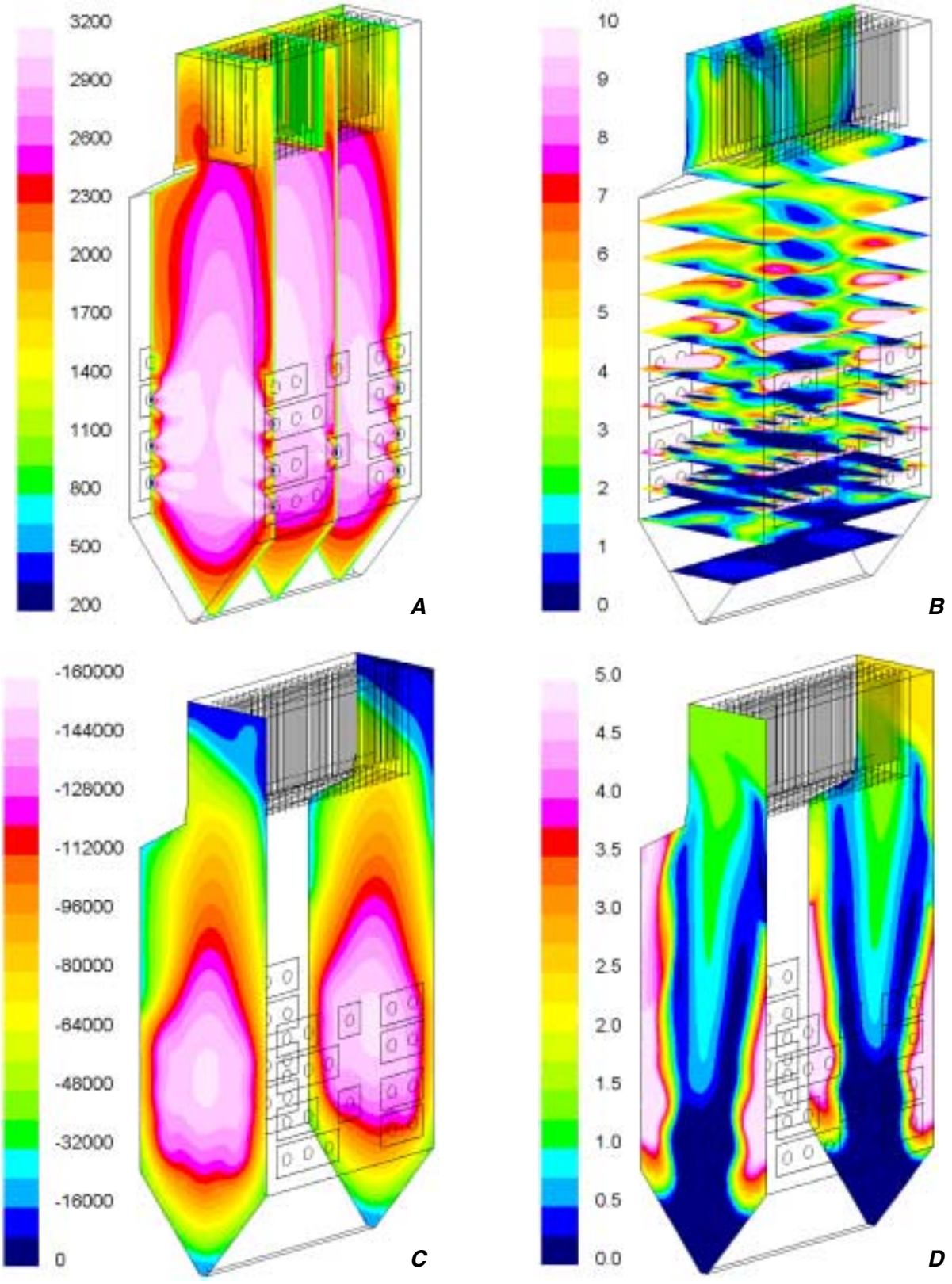

Figure 12a, b, c, and d. Computed furnace gas temperature, furnace gas O_2 concentration, sidewall heat flux, and sidewall O_2 concentration distributions in a wall-fired furnace for the existing firing system before retrofit of new RPI dual air zone CCV® Burners and OFA.

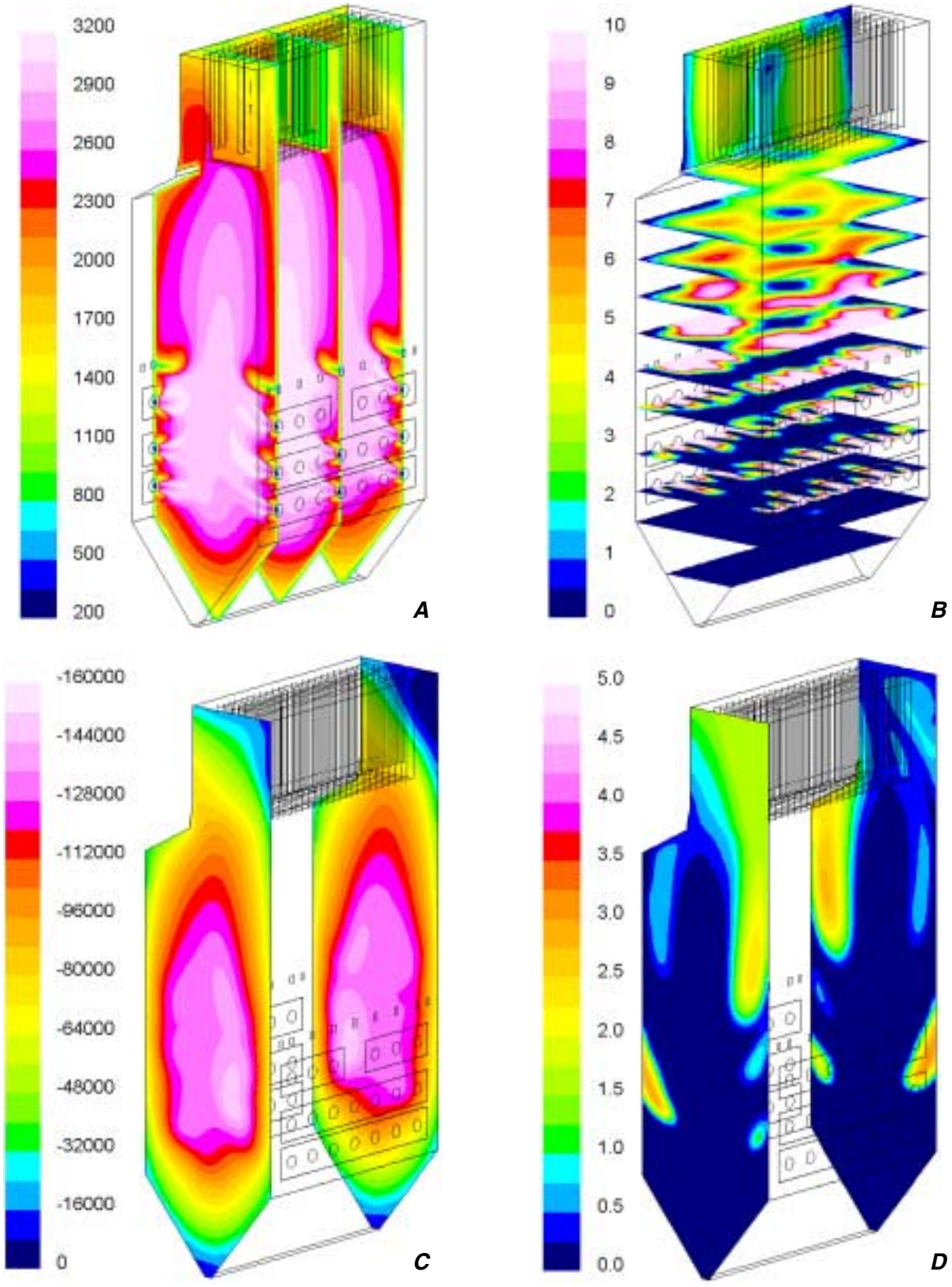

Figure 13a, b, c, and d Computed furnace gas temperature, furnace gas O_2 concentration, sidewall heat flux, and sidewall O_2 concentration distributions in a wall-fired furnace with retrofit of new RPI dual air zone CCV® Burners and OFA system.

Even though the design employs furnace air staging, thus shifting the firing zone from above stoichiometric to substoichiometric, Figures 12 and 13 suggest no significant shift in the pattern of sidewall O_2 amount in relation to regions of highest wall heat flux. This is an important issue since high wall heat flux with very low wall O_2 potentially increases wall wastage, which historically has been at the sidewall center at and above the top two burner rows, just as shown in the CFD results. The customer decided to extend the CFD project to investigate possible boundary air designs to increase O_2 along the sidewalls in anticipation of corrosion problems. Figure 14 shows CFD model results for the two major options: a) boundary air ports on the firing walls, and b) sidewall boundary air slots which take advantage of the unit's membrane wall construction. The port approach uses more combustion air applied in the burner zone thus increasing burner zone stoichiometry and increasing NOx, while the slot system uses only a small amount of combustion air applied directly to the sidewalls where needed most. Figure 14 shows the performance of the slot approach will be significantly greater than the port approach, even if no further optimization of slot location is done beyond this initial attempt.

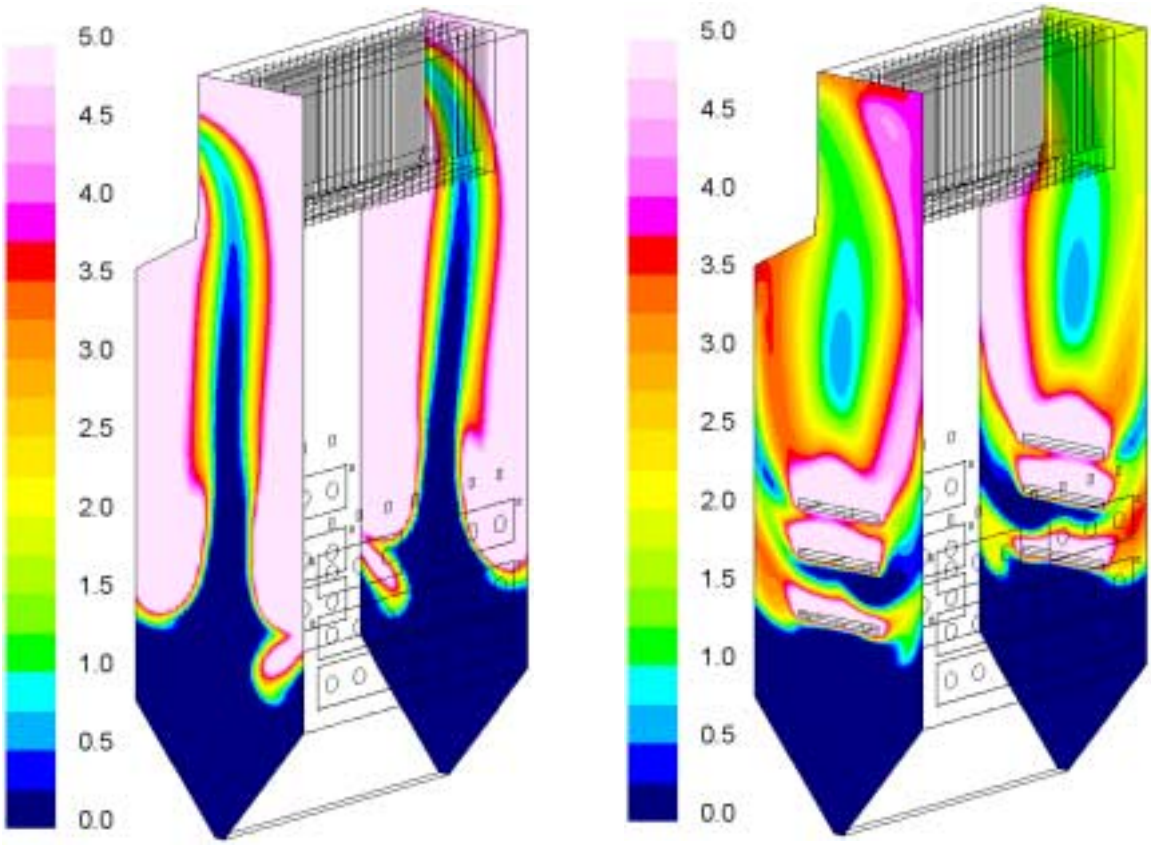

Figure 14 Computed sidewall O_2 distributions for initial sidewall boundary air designs: left, four upper and four lower firing wall ports, and right, mid-sidewall slots at three levels.

This project illustrated the value of CFD to provide support for engineering decisions such as reconfiguring a firing system layout and the choice of coordinated OFA design for proper upper furnace mixing, temperature control, and emissions reduction. The economic impact of the CFD process appeared as a short startup and guarantee test period with almost no problems.

INDUSTRIAL BOILERS

Although CFD simulations of large utility furnaces most often are 3-D as noted above, simpler 2-D CFD modeling can be equally effective in producing useful results in some furnace problems, especially for industrial or package boilers. One virtue of using simple 2-D CFD models is speed in obtaining answers compared to large 3-D furnace models.

Figure 15 shows the CFD 2-D model geometry, computed gas temperature and velocity distributions in an industrial boiler at an industrial facility with multiple boilers firing process off gases to raise steam to a common steam line. As part of the plant's emissions

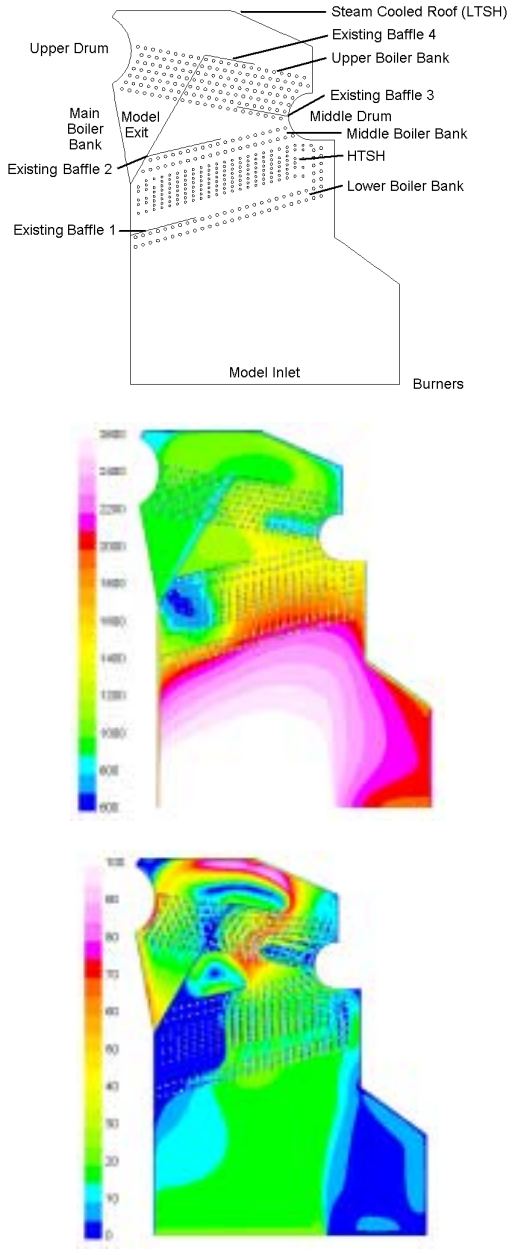

Figure 15 CFD 2-D model and computed temperature and velocity distributions for base case (existing furnace).

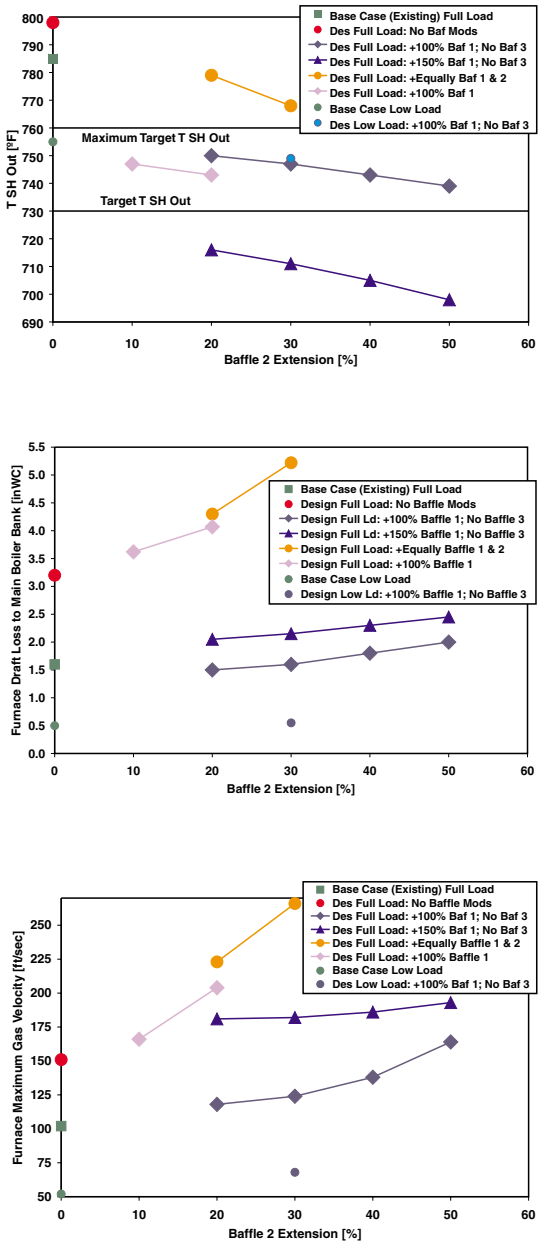

Figure 16 CFD-derived system performance curves: SH steam out, draft loss, and maximum gas velocity

control plan, the boilers received, in a phased retrofit, new low NO_X burners employing significant flue gas recirculation (FGR) and steam injection. The boiler gas mass flows increase due to the FGR and thus increase steam outlet temperatures above the maximum allowed value if no boiler modifications were made. The project goal was to modify existing baffles in one boiler to control its full- and low-load final steam temperatures within a narrow range with a minimal rise in boiler draft loss.

The models become even simpler by leaving out combustion but including convective and radiation heat transfer to allow quick determination of parametrically related boiler performance curves such as in Figure 16 for final steam temperature, furnace draft loss, and peak gas velocity as an indicator of erosion potential. Model calibration to baseline field data accounted for 3-D effects such as the sidewalls and lower furnace. In this approach, an individual model is significant only as a point in the performance curves rather than as the result itself. Performance curves show design options and allow adjustment of a solution to changes in the problem. For example, it turned out that actual baffle lengths were different from the drawings, and after restart the steam pressure was lower than design because the main boiler was off line. As a result, the originally proposed solution reduced steam temperature too much, but the performance curves indicated the size of a correction with no additional simulations needed. However, to reduce total costs, the plant may not correct the low steam outlet temperature, but use it to attemperate output of other boilers getting the new burners but possibly no baffle modifications.

In this example the customer received significant economic value from the simple 2-D CFD modeling approach. Project execution time, including simulation and reporting tasks, was only 8 days due to the simple, fast-computing 2-D models. The project cost was very low and delivery of results kept pace with the fast-track work at the site. Additionally, the approach produced system performance maps with real engineering utility and life well beyond the project. With the performance maps the customer can design furnace modifications for steam temperature control for many years without additional expenditures for outside engineering.

AIRHEATERS TO ESPs

Under the pressures to reduce fuel costs, extend the range of fuel quality that may be fired, or fire a fuel that helps reduce a plant's emissions, a utility may choose to switch from one coal type to another. Sometimes this fuel switch can have unintended consequences. For example, the new coal may produce an ash with different electrochemical properties like resistivity, and once-functioning ESPs no longer work correctly.

The ductwork between the airheater and the ESPs is the only place to fit in a solution, in this case an injection station to spray a conditioning agent into the flue gas to shift ash resistivity back to a range good for the ESPs. The spray system actually created the problem in this example of a 448 MW coal-fired unit, since the spray required a flue gas temperature variation across the duct less than 70ºF at 114% MCR, while the existing distribution was about 125ºF at 100% MCR leaving the large, multi-pass tubular airheater. Thus a need arose for the design of a flue gas mixing system between the airheater cold gas outlet and the spray station. Additional constraints included: 1) No modification of existing ductwork. 2) Draft loss increase <1.0 iwc. 3) Ground up radial tires are mixed into the coal, which creates significant large steel fluff in the flyash. 4) A water spray wash system in the airheater exit hood must remain functional. 5) Mixed flue gas temperature leaving the airheater > 320ºF to avoid acid condensation in the ductwork. Possible solution approaches included: 1) Take advantage of flow stratification within the multi-pass airheater. 2) Do all the mixing at the last instant before the spray station. 3) Improve flow details within and around the airheater. 4) Combine all of these.

In some respects this is an awkward problem for solution by CFD modeling because it is too cumbersome to solve all at once due to the large multi-pass tubular airheater and the varied nature of solution approaches. The airheater exit gas distribution depends on the hot gas flow distribution into the airheater, the air distribution into the airheater, and the performance of the multi-pass airheater itself. Figure 17 shows the four separate CFD models used in a segmented but coupled solution technique, which became an advantage. The separate models concentrated on flow behavior outside the tube bundle cores, and a custom program for hot and cold bundle section heat transfer performance coupled the inputs and outputs of the CFD models as shown in Figure 18. This approach eliminated CFD modeling difficulties due to the large tube counts in the airheater cores. It also allowed quick coupling of different inlet models, hopper models, and outlet models to assess local and global changes in performance.

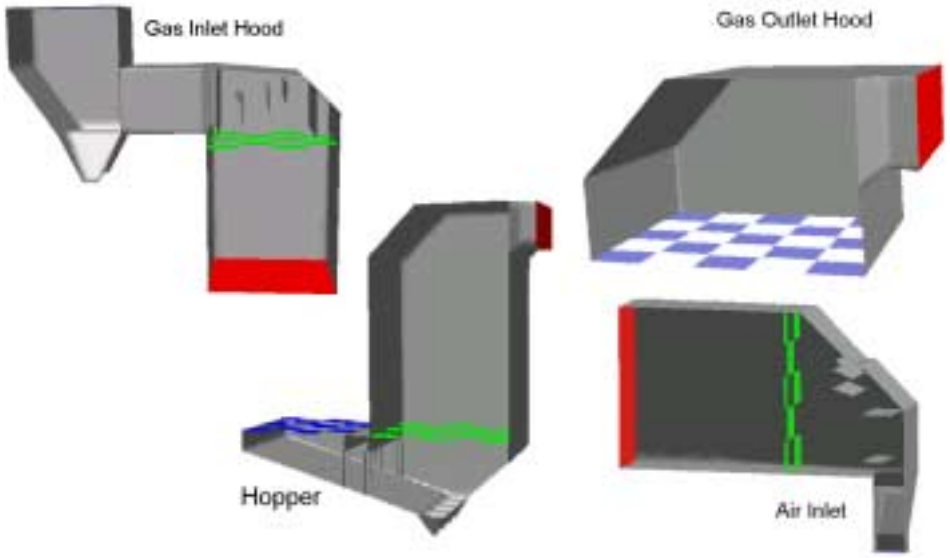

Figure 17 Four separate but coupled CFD models for tubular air heater problem.

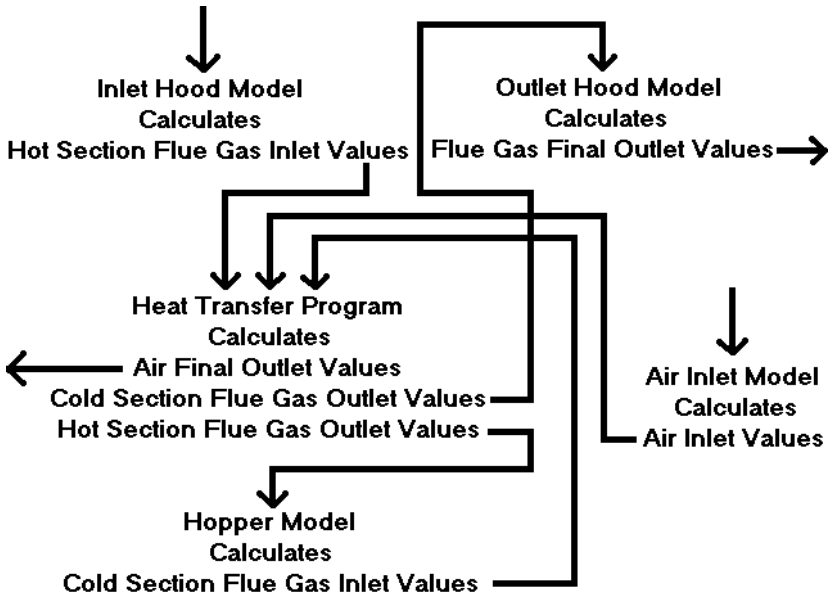

Figure 18 Technique for coupling separate CFD models and heat transfer calculations.

Figure 19 shows computed results for the original airheater system and the proposed solution using a large-scale riffle plate system in the exit hood for flue gas mixing at the last instant combined with attention to details elsewhere in the system: 1) Perforated plate in the air inlet to improve air mass flow distribution into the airheater. 2) Fairings connecting support pillars in the hopper to improve flue gas temperature stratification from hot to cold section. The models predict a 62ºF exit flue gas temperature variation, a 1.9 iwc draft loss increase, and a more uniform hot air exit distribution. Limited acceptance testing measured a 60ºF temperature variation, and the draft loss was either not noted or not a significant issue.

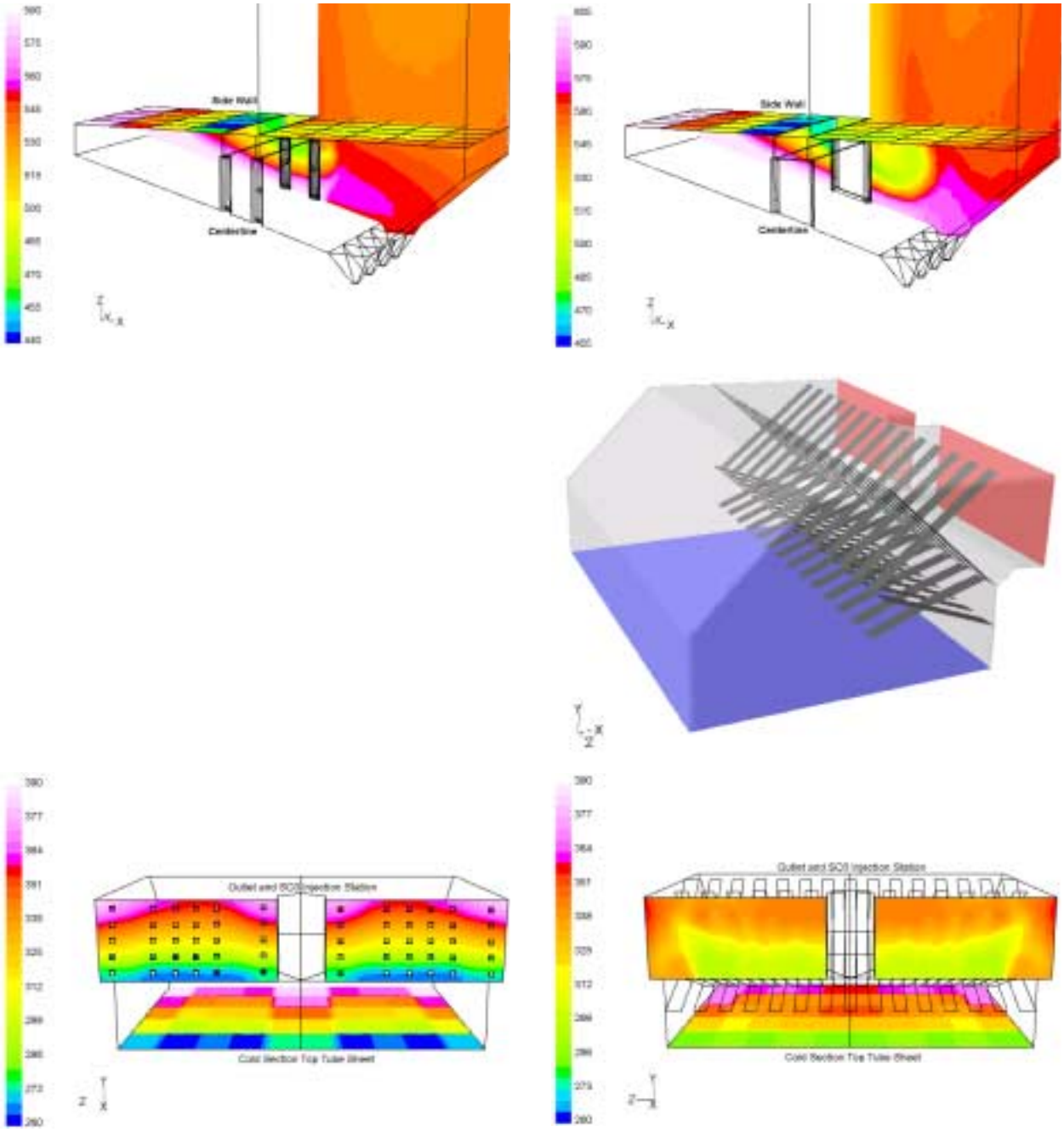

Figure 19 Computed gas temperature results in hopper, inlet of turning hood, and inlet to spray location for original system (left) and CFD-derived solution (right).

Here it is hard to estimate the value of the CFD, since the CFD-derived design simply performed as required and was obtained within the tight schedule given. The CFD models did highlight why and where the existing outlet temperature variations were so high for both cold gas and hot air leaving the airheater. Thus the CFD modeling pointed to places for simple and inexpensive improvement that otherwise might be overlooked, which would have led to more expensive and less effective implementations.

SCR SYSTEMS

With the advent of ever-tightening emissions requirements, many coal-fired utility boilers include an SCR system after the backpass heat transfer section and before any other gas cleanup equipment. The SCR system removes NO_X from the hot flue gas stream by catalytically enhanced chemical reactions. The catalysts in the SCRs are sensitive to gas temperature, velocity, and particulate loading as well as the distributions of these quantities entering the SCR reactor.

In the example presented here, several stages of proprietary RPI static mixers give a near-uniform flue gas flow into the SCR as required by the catalyst. Unfortunately, combustion in the boiler's furnace and action of the catalyst can generate an unwanted trace species which leads to problems in the boiler's stack plume. A cost-effective approach to solving this problem is a water spray-based flue gas attemperator system in the ductwork leading to the SCR reactor. Water is readily available and cheap, and through its large latent heat of vaporization, a small amount of water spray can trim flue gas temperature enough to reduce the unwanted species without degrading catalyst performance too much. Physical access constrains the spray system location to a point just downstream of the first static mixer stage, which induces large-scale gas motion and high turbulence levels in the duct. Therefore, a basic "even spray pattern" may not be the best choice since water spray wetting of the duct walls leads to acid formation and rapid corrosion of the ductwork. Quick CFD modeling provides an opportunity to customize the spray pattern design to accomplish two objectives: 1) Reduce wetting of the duct walls by the sprays. 2) Distribute the water and its cooling effect within the ductwork so as to maintain or improve the gas temperature profile entering the SCR reactor.

Figure 20 shows the computed temperature distribution for a base case with no spray flow as a benchmark of mixer behavior. The temperature distribution at the model exit agreed well with limited field data. Figure 21 shows computed results of temperature and water vapor concentration for a field test that took place just before the CFD model calculations. Temperature measurements during the field test showed a worse distribution than without the spray, and the test system was removed. The model results in Figure 21 agreed with the test field measurements. The CFD results showed that the hot and cold gas regions shifted location and the temperature distribution widened because the test spray did not fill the duct cross-section but remained close to the roof after injection. Figure 22 shows the computed results for a custom-designed spray nozzle layout case chosen for minimum wall wetting by unevaporated spray. Figure 22 indicates the suggested spray pattern not only attains the goal of trimming gas bulk temperature but also makes the temperature distribution more even than without the spray. This is quite an improvement over the field test results.

In this case almost $100,000 was spent on a field test before the CFD simulation that showed the test would give the poor results it actually did. Perhaps worse than the cost of a failed field test was the possible perception that a viable solution approach was now seen as worthless. This could have led to other more expensive, and less effective attempts to solve the problem.

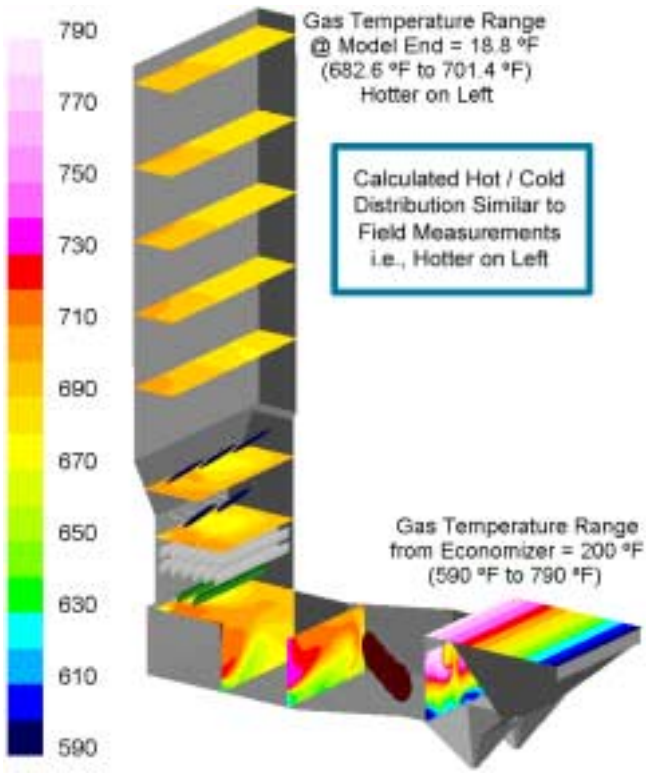

Figure 20 Computed temperature distribution for base case (no water spray).

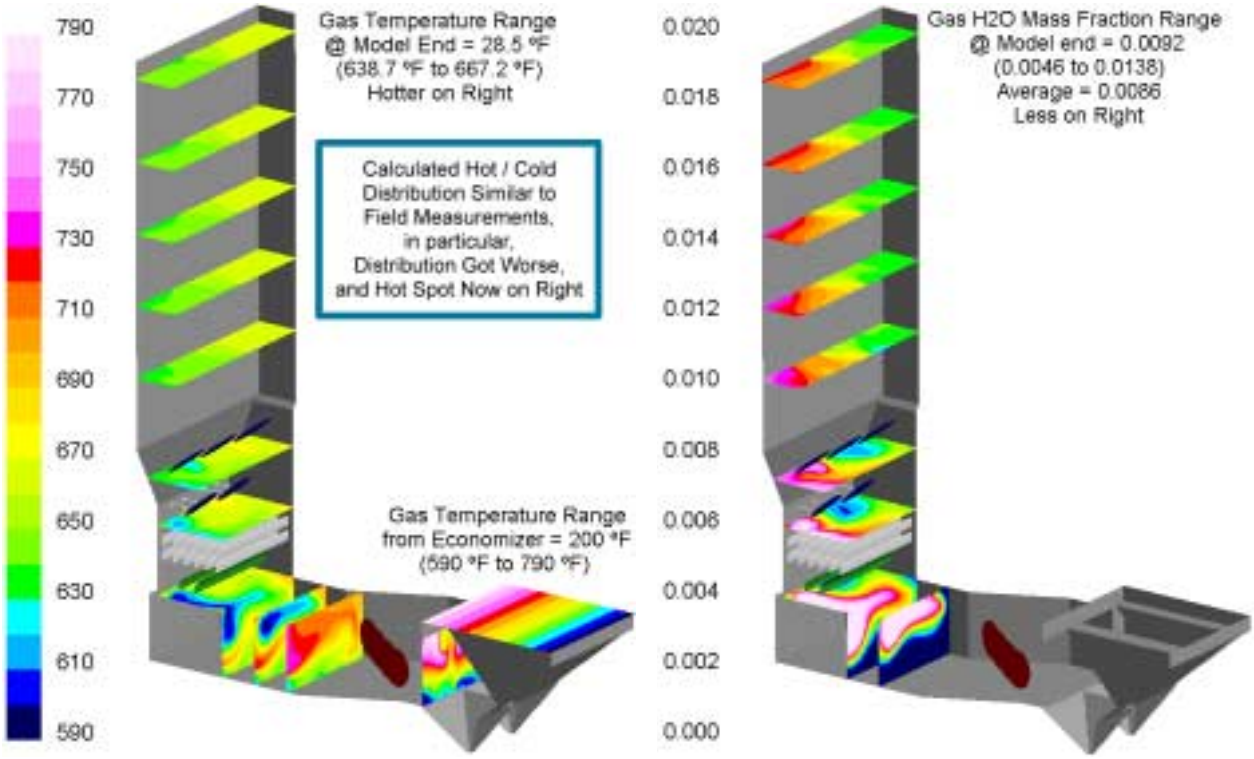

Figure 21 Computed temperature and water vapor distributions for field test startup.

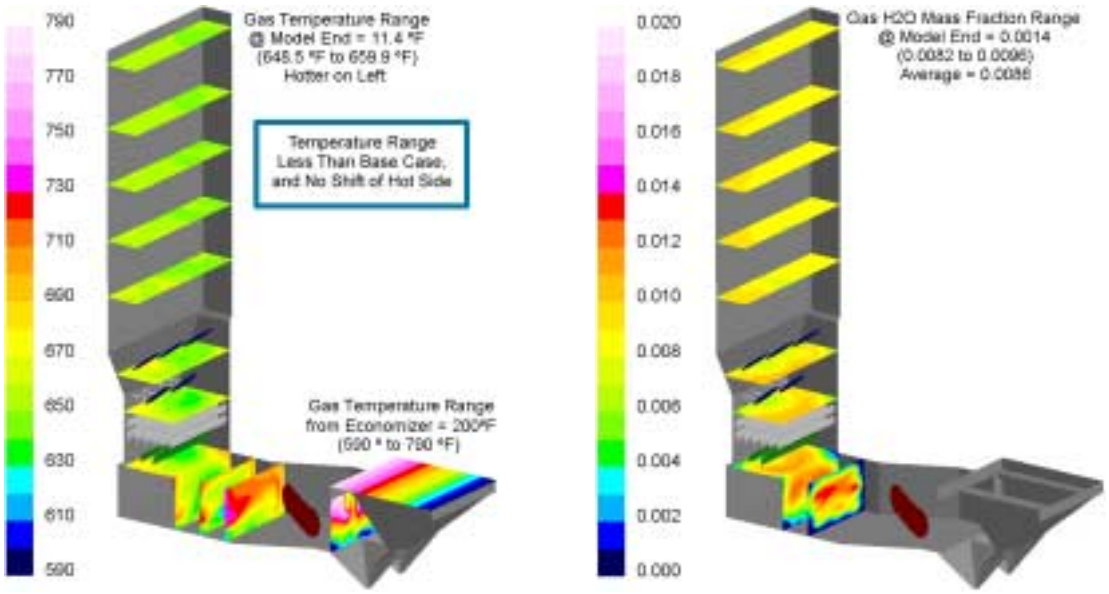

Figure 22 Computed temperature and water vapor distributions for recommended setup.

SUMMARY

This survey of recent RPI CFD projects is not exhaustive, but it does show that CFD can be an important engineering tool in the power industry. CFD can give useful, practical results of significant economical benefit about questions or problems covering traditional power generation equipment as well as new environmentally oriented systems, literally from bunker to stack.

The examples above often featured simple 2-D CFD models rather than large 3-D models, which can turn into academic tours-de-force rather than cost effective engineering solutions. When applicable, simple 2-D CFD models have three virtues: speed, range, and maps of system performance or behavior. Simple 2-D models can cover a very wide range of operating conditions and geometry changes very quickly compared to large 3-D models. Then the wide range of calculated results may be assembled into trends dependent on key geometry and operating conditions as parameters. Performance maps provide useful insight into system behavior and practical direction for modifying a system to obtain desired control and output.

No claim is made or implied, however, that CFD can solve all problems in power plant equipment and systems. CFD is only one of many tools for solving engineering problems and making economically advantageous improvements. All parties in a CFD project need to remain cautious about the CFD calculations. CFD codes are now robust so they almost always give a "result," which may or may not be an "answer" to the problem. Successful CFD projects should include 1) acquisition of quality, reliable field test data for one or more baseline cases and 2) validation of the CFD models against these data. Good baseline data is not an extra cost of the CFD process, since any serious plan to solve a problem or make improvements, even by expensive field testing methods, needs a reliable starting point to measure progress. In the CFD approach, if the base case CFD models do not agree well enough with the baseline data, then the CFD process should stop. If there is satisfactory agreement between models and baseline data, then the CFD process can proceed. Now there is more confidence among all parties that the results of new CFD models, which are exploring changes in geometry and conditions, have merit.

The data contained herein is solely for your information and is not offered,
or to be construed, as a warranty or contractual responsibility.